Mesh-adaptive computation of linear and non-linear acoustics

Anca Belme(*), Alain Dervieux(*) and Frédéric Alauzet(**)

(*)INRIA - Tropics project Sophia-Antipolis, France
(**)INRIA - Gamma Project Rocquencourt, France
Anca.Belme@sophia.inria.fr

CEAA 2010

Svetlogorsk, September 22-25 2010

1. Anisotropic mesh adaptation
2. Anisotropic goal-oriented mesh adaptation
3. Extension to unsteady
4. Applications to blast waves
5. Applications to linear acoustics

Riemannian metric space: $(\mathcal{M}(\mathbf{x}))_{\mathbf{x}\in\Omega}$

- Distance:

$$\text{Distance}(a,b) = \ell_{\mathcal{M}}(\mathbf{ab}) = \int_0^1 \sqrt{{}^t\mathbf{ab}\ \mathcal{M}(\mathbf{a}+t\mathbf{ab})\ \mathbf{ab}}\,\mathrm{d}t$$

- Complexity $\mathcal{C}$:

$$\mathcal{C}(\mathbf{M}) = \int_\Omega d(\mathbf{x})\,d\mathbf{x} = \int_\Omega \sqrt{\det(\mathcal{M}(\mathbf{x}))}\,d\mathbf{x}.$$

- Matrix writing:

$$\mathcal{M}(\mathbf{x}) = d^{\frac{2}{3}}(\mathbf{x})\,\mathcal{R}(\mathbf{x}) \begin{pmatrix} r_1^{-2/3}(\mathbf{x}) & & \\ & r_2^{-2/3}(\mathbf{x}) & \\ & & r_3^{-2/3}(\mathbf{x}) \end{pmatrix} {}^t\mathcal{R}(\mathbf{x}).$$

- **Main idea:** change the distance evaluation in the mesh generator
  [Vallet, 1992], [Casto-Diaz et Al., 1997], [Hecht et Mohammadi, 1997]

- **Fundamental concept: Unit mesh**

Adapting a mesh

$\Updownarrow$ Work in adequate Riemannian metric space

Generating a uniform mesh w.r.t. to $\mathcal{M}(\mathbf{x})$

$$\mathcal{H} \text{ unit mesh} \iff \forall \mathbf{e},\ \ell_{\mathcal{M}}(\mathbf{e}) \approx 1 \text{ and } \forall K,\ |K|_{\mathcal{M}} \approx \begin{cases} \sqrt{3}/4 & \text{in 2D} \\ \sqrt{2}/12 & \text{in 3D} \end{cases}$$

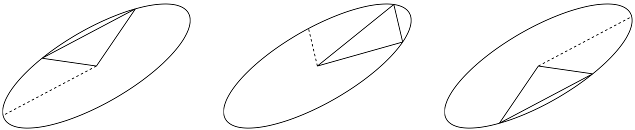

For any K which is unit for $\mathcal{M}$ and for all u quadratic positive form ($u(\mathbf{x}) = \frac{1}{2}\,{}^t\mathbf{x}\,H\,\mathbf{x}$):

$$\|u - \Pi_h u\|_{\mathbf{L}^1(K)} = \frac{\sqrt{2}}{240}\, \underbrace{\det(\mathcal{M}^{-\frac{1}{2}})}_{\textit{mapping}}\, \underbrace{\operatorname{trace}(\mathcal{M}^{-\frac{1}{2}}\, H\, \mathcal{M}^{-\frac{1}{2}})}_{\textit{anisotropic term}}$$

Continuous interpolation error:

$$\forall \mathbf{x} \in \Omega\,, \quad |u - \pi_{\mathcal{M}} u|(\mathbf{x}) \;=\; \frac{1}{10}\operatorname{trace}\left(\mathcal{M}(\mathbf{x})^{-\frac{1}{2}}\, |H(\mathbf{x})|\, \mathcal{M}(\mathbf{x})^{-\frac{1}{2}}\right)$$

equivalent because:

$$\frac{1}{10}\operatorname{trace}\left(\mathcal{M}(\mathbf{x})^{-\frac{1}{2}}\, |H(\mathbf{x})|\, \mathcal{M}(\mathbf{x})^{-\frac{1}{2}}\right) \;=\; 2\,\frac{\|u - \Pi_h u\|_{\mathbf{L}^1(K)}}{|K|}$$

for any K which is *unit* with respect to $\mathcal{M}(\mathbf{x})$.

We proposed a continuous mesh framework to solve this problem

Discrete	**Continuous**
Element K	Metric tensor $\mathcal{M}(\mathbf{x}_K)$
Mesh $\mathcal{H}$ of Ω_h	Riemannian metric space $\mathcal{M} = (\mathcal{M}(\mathbf{x}))_{\mathbf{x}\in\Omega}$
Number of vertices N_v	Complexity $\mathcal{C}(\mathcal{M}) = \int_\Omega \sqrt{\det(\mathcal{M}(\mathbf{x}))}\, d\mathbf{x}$
Linear interpolate $\Pi_h u$	**Continuous linear interpolate** $\pi_\mathcal{M} u$

We call multi-scale adaptation the minimisation of the L^p-norm, with $p < \infty$, of the continuous interpolation:

Find $\mathbf{M}_{opt} = (\mathcal{M}_{opt}(\mathbf{x}))_{\mathbf{x}\in\Omega}$ of complexity N such that

$$\begin{aligned} E_{\mathcal{M}_{opt}}(u) &= \min_{\mathcal{M}} \|u - \pi_{\mathcal{M}} u\|_{\mathcal{M},\mathbf{L}^p(\Omega)} \\ &= \min_{\mathcal{M}} \left(\int_{\Omega} |u(\mathbf{x}) - \pi_{\mathcal{M}} u(\mathbf{x})|^p \,\mathrm{d}\mathbf{x} \right)^{\frac{1}{p}} \end{aligned}$$

A well-posed problem solved by a calculus of variations.

Optimal metric

$$\mathcal{M}_{\mathbf{L}^p} = \underset{❶}{D_{\mathbf{L}^p}} \quad \underset{❷}{\left(\det|H_u|\right)^{\frac{-1}{2p+3}}} \quad \underset{❸}{\mathcal{R}_u^{-1}} \quad \underset{❹}{|\Lambda|} \quad \mathcal{R}_u$$

❶ Global normalization: to reach the constraint complexity N

$$D_{\mathbf{L}^p} = N^{\frac{2}{3}} \left(\int_\Omega (\det|H_u|)^{\frac{p}{2p+3}} \right)^{-\frac{2}{3}} \quad \text{and} \quad D_{\mathbf{L}^\infty} = N^{\frac{2}{3}} \left(\int_\Omega (\det|H_u|)^{\frac{1}{2}} \right)^{-\frac{2}{3}}$$

❷ Local normalization: sensitivity to small solution variations, depends on $\mathbf{L}^p$ norm chosen

❸ Optimal anisotropy directions based on Hessian eigenvectors

❹ Diagonal matrix of anisotropy strengths, defined from the absolute values of Hessian eigenvalues

Fixed point algorithm

- Compute flow
- Compute metric field
- Build new mesh
- Interpolate old data on new mesh

Background and properties:

[Castro Diaz *et al.*, 1997], [Habashi *et al.*, 2000], [Frey and Alauzet, 2005], ...

- Genericity, does not depend on the PDE and on the numerical scheme
- Anisotropy easily deduced
- The multiscale (*i.e.* L^p) version provides an optimal mesh without neglecting weaker details.

An example: supersonic steady flow around an aircraft.

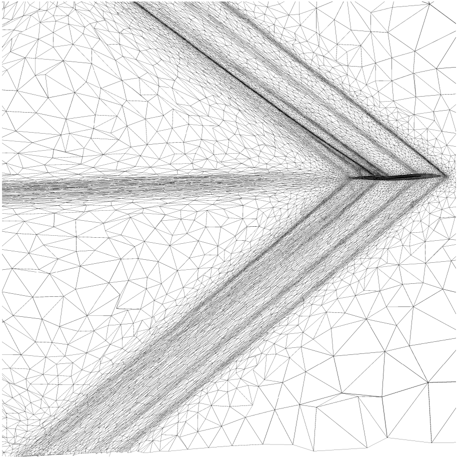

Objectif

Deriving the best mesh to observe a given functional $j(w) = (g, w)$ depending of the solution w of a PDE and enough regular to be observed through its Jacobian g.

How?

Control of the approximation error on the output functional : $j(w) - j(w_h)$.

Exemples

- vorticity in wake $j(\mathbf{w}) = \int_\gamma \|\nabla \wedge (\mathbf{u} - \mathbf{u}_\infty)\|_2^2 \, d\gamma$
- drag, lift: use to quantify the performance of a design , etc...

Background:

[Becker-Rannacher],[Giles-Pierce],[Venditti-Darmofal, 2002],[Rogé-Martin, 2008],. . .

- Explicit use of the PDE
- Strong dependency on the numerical scheme
- Anisotropy hard to prescribe

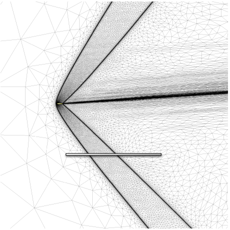

- Given a functional $j(w)$
- We only know w_h
- How to control $j(w) - j(w_h)$

Continuous and discrete equations

$$(\Psi(w), \phi) = 0 \quad \text{and} \quad (\Psi_h(w_h), \phi_h) = 0$$

Continuous and discrete adjoint equations

$$(\frac{\partial \Psi}{\partial w}(w)\phi, w^*) = (g, \phi) \quad \text{and} \quad (\frac{\partial \Psi_h}{\partial w}(w_h)\phi_h, w_h^*) = (g, \phi_h)$$

Adjoint estimation

- Dual formula [Giles et Süli, 2002]

$$j(w) - j(w_h) \approx (g, w - w_h) \;=\; \underbrace{-(w^*, \Psi(w_h))}_{A\ posteriori} \;=\; \underbrace{(w_h^*, \Psi_h(w))}_{A\ priori}$$

A priori error estimation [A. Loseille and A. Dervieux and F. Alauzet, Fully anisotropic goal-oriented mesh adaptation for 3D steady Euler equations, JCP, 2010]

$$j(w) - j(w_h) = \underbrace{(g, w - w_h)}_{\textit{Approximation error}} = \underbrace{(g, w - \Pi_h w)}_{\textit{Interpolation error}} + \underbrace{(g, \Pi_h w - w_h)}_{\textit{Implicit error}}$$

$$= \big((\Psi_h - \Psi)(w), w_h^*\big) + R_3$$

- Search for continuous model $E(\mathcal{M})$ to evaluate $(\Psi_h - \Psi)(w)$.
- Find $\mathcal{M}$ that minimises $\big(E(\mathcal{M}), w^*\big)$.

Application to sonic boom :

- Adjoint functional :

$$j(W) = \int_{\gamma} \left(\frac{p - p_{\infty}}{p_{\infty}} \right)^2 \, \mathrm{d}\gamma$$

- Adaptation variable : Mach number

2. Goal-oriented mesh adaptation: application

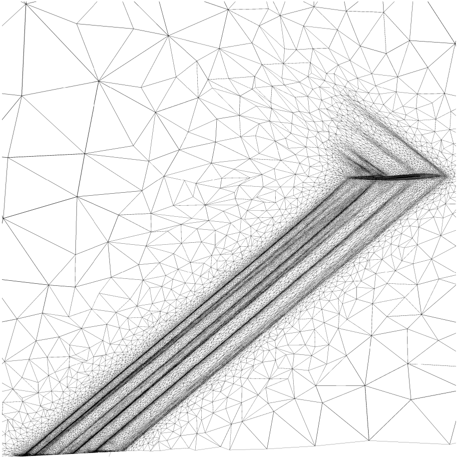

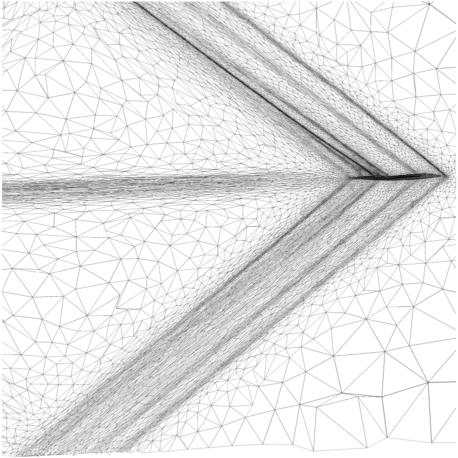

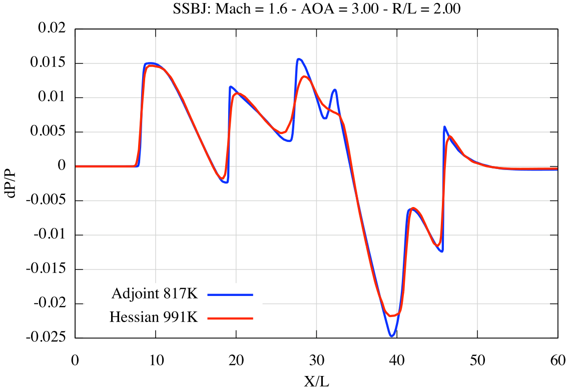

Even close to the aircraft (2 lengths), the adjoint-based adaptation strongly supersedes the multiscale method.

Problematics:

- Evolution of physical phenomena in time.
- One may need a good prediction of solution evolution into the whole computational domain. In this case, the unsteady multiscale method need be applied. We refer to Alauzet *et al.* JCP (2007).
- A target observation can be specified: the goal oriented version is needed.
- We neglect time-discretisation errors in the present study.

$$(\Psi(W),\Phi) = \int_Q \Phi\ \partial_t W \,\mathrm{d}Q + \int_Q \Phi\ \nabla.\mathcal{F}(W)\,\mathrm{d}Q - \int_\Sigma \Phi\ \hat{\mathcal{F}}(W)\,\mathrm{d}\Sigma$$

$$(\Psi_h(W),\Phi_h) = \int_Q \Phi_h\ \Pi_h\partial_t W \,\mathrm{d}Q + \int_Q \Phi_h \nabla.\Pi_h\mathcal{F}(W)\,\mathrm{d}Q - \int_\Sigma \Phi_h\Pi_h\hat{\mathcal{F}}(W)\,\mathrm{d}\Sigma$$

with $Q = \Omega \times]0, T[$, $\Sigma = \partial\Omega \times]0, T[$.

Let:

$$j(w) = (g, w)_Q$$

$$j(w) - j(w_h) \approx \int_Q W^*\ (\partial_t W_h - \partial_t W + \nabla.\mathcal{F}_h(W) - \nabla.\mathcal{F}(W))\,\mathrm{d}Q + \mathrm{BT}$$

$$= \int_Q W^*\ (\partial_t W_h - \partial_t W)\,\mathrm{d}Q + \int_Q \nabla.W^*\ (\mathcal{F}(W) - \mathcal{F}_h(W))\,\mathrm{d}Q + \mathrm{BT}$$

$$= \int_Q W^*\ (\Pi_h\partial_t W - \partial_t W)\,\mathrm{d}Q + \int_Q \nabla.W^*\ (\mathcal{F}(W) - \Pi_h\mathcal{F}(W))\,\mathrm{d}Q + \mathrm{BT}$$

Boundary integrals ("BT") are tranformed in a similar manner.

Solve this problem in the continuous framework

Find $\mathbf{M}_{opt} = (\mathcal{M}_{opt}(\mathbf{x}))_{\mathbf{x}\in Q}$ of complexity N such that

$$E(\mathcal{M}_{opt}) = \min_{\mathcal{M}} \Big(\int_Q W^* \, (\pi_{\mathcal{M}} W_t - W_t)\, \mathrm{d}Q + \int_Q \nabla . W^* \, (\mathcal{F}(W) - \pi_{\mathcal{M}} \mathcal{F}(W))\, \mathrm{d}Q + \mathrm{BT} \Big)$$

A calculus of variations gives

$$\mathcal{M}_{opt} = \mathcal{M}_{opt}^{\mathbf{L}^1} \left(\sum_{i=1}^{5} (|W_h^*(W_i)|\, |H(W_{i,t})| + \sum_{j=1}^{3} |\nabla_{x_j} W_h^*(W_i)|\, |H(\mathcal{F}_{x_j}(W_i))|) \right)$$

Discrete State System and functional:

$$\Psi_h^{n+1}(W^n, W^{n+1}, \phi^n) = 0 \Leftrightarrow W = W_{sol}$$

$$j = J(W_{sol})$$

Discrete Adjoint State System writes:

$$W^{*,N} = \left(\frac{\partial \Psi_h^N}{\partial W^N}\right)^{-T} \left(\frac{\partial J}{\partial W^N}\right)^T$$

$$W^{*,n} = \left(\frac{\partial \Psi_h^n}{\partial W^n}\right)^{-T} \left[\left(\frac{\partial J}{\partial W^n}\right)^T - \left(\frac{\partial \Psi_h^{n+1}}{\partial W^n}\right)^T W^{*,n+1}\right] \forall\ n = \overline{N-1, 0}$$

$\Longrightarrow$ Adjoint State is computed backwards in time.

Adjoint is advanced forward in time:

- Computing $W^{*,n}$ from the adjoint state $W^{*,n+1}$ needs the knowledge of states W^n, W^{n+1} .
- Higher-Order scheme with intermediate storage (like explicit Runge-Kutta schemes) demands even more storage/recompute effort

Our approach:

- Storage of the solution on checkpoints $\Longrightarrow$ forward/backward computation only between two checkpoints.
- Interpolate Adjoint states between two adaptation sub-intervals.

Optimal Metric computation needs:

- Adjoint state : W^* (computed backwards in time)
- Adjoint state gradient : $\nabla\ W^*$
- Hessian of the Euler fluxes : $H(\mathcal{F}(W))$
- Hessian of time derivative: $H(W_t)$

Continuous states $\Longleftarrow$ approximated by the discrete ones

Gradients and Hessians $\Longleftarrow$ derivative recovery (L^2 -projection)

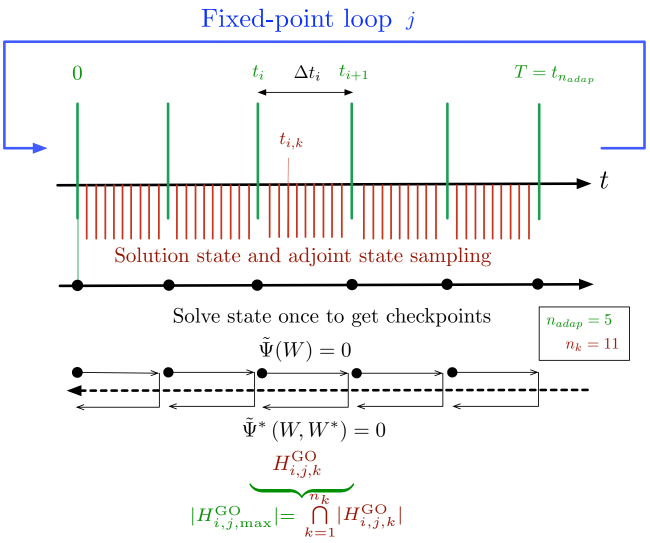

Fixed-point loop j
0
t_i
Δt_i
t_{i+1}
$T = t_{n_{adap}}$
$t_{i,k}$
t
Solution state and adjoint state sampling
Solve state once to get checkpoints
$n_{adap} = 5$
$n_k = 11$
$\tilde{\Psi}(W) = 0$
$\tilde{\Psi}^*(W, W^*) = 0$
$H^{GO}_{i,j,k}$
$|H^{GO}_{i,j,\max}| = \bigcap_{k=1}^{n_k} |H^{GO}_{i,j,k}|$

Blast-like initialisation inside a circle of radius $r_0 = 0.15$ around $x_0 = (1.2, 0.0)$, given by: $\rho = 10.0$, $v = (0, 0)$ and $e = 25.0$.

The cost function j was the impulse over the target surface S in Figure below:

$$j(W) = \frac{1}{2}\int_S (p - p_\infty)^2 ds.$$

Figure: Channel flow 2D mesh

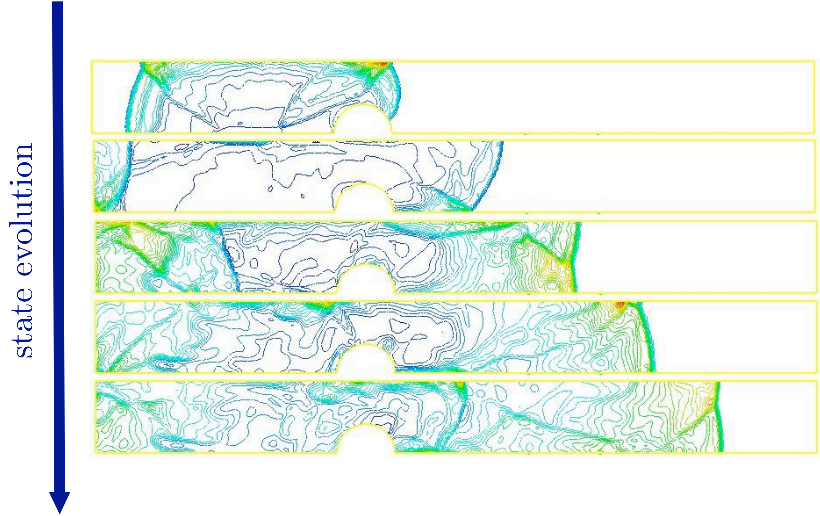
state evolution

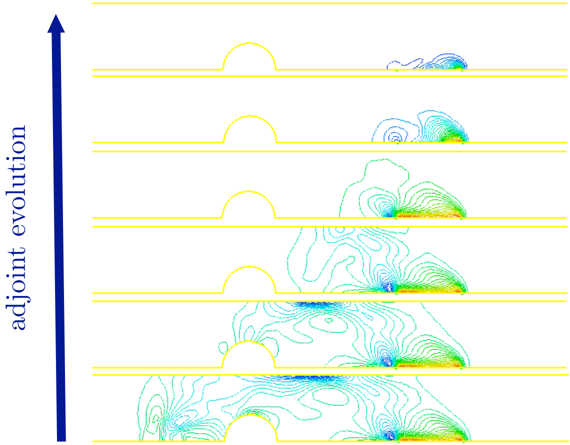
adjoint evolution

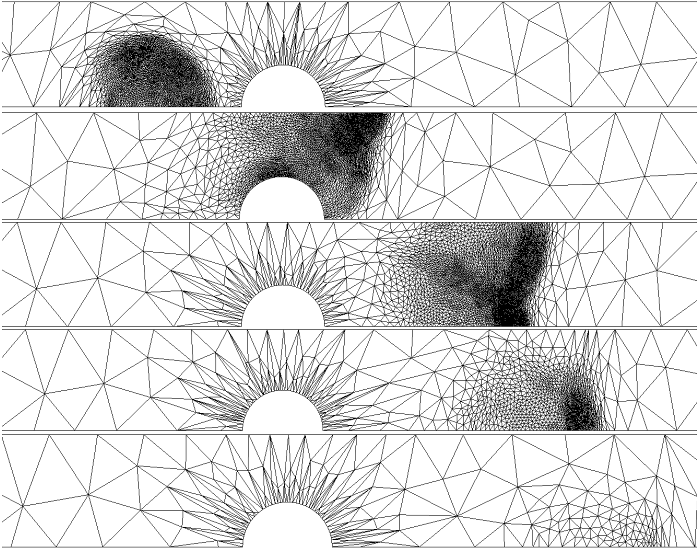

Second Example

Nonlinear “blast” wave.

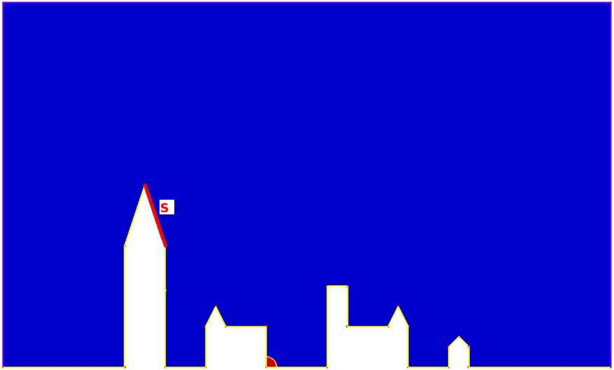

Second Example, results

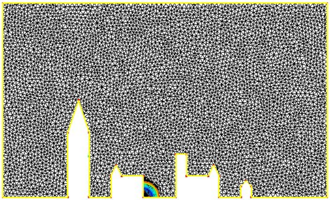

Second Example, results

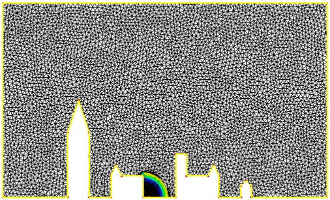

Second Example, results

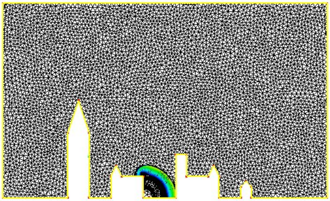

Second Example, results

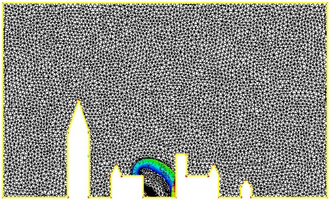

Second Example, results

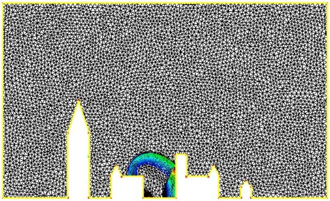

Second Example, results

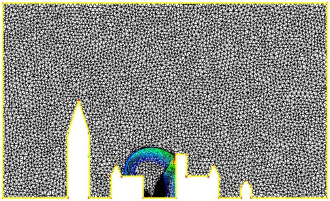

Second Example, results

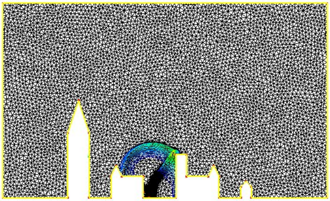

Second Example, results

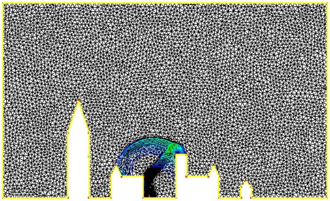

Second Example, results

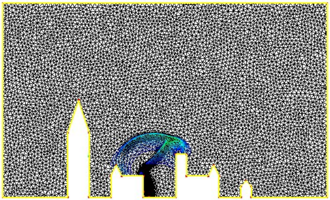

Second Example, results

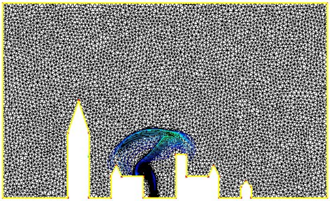

Second Example, results

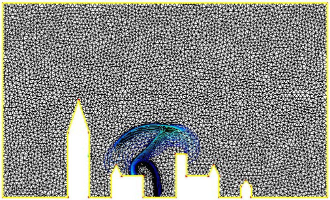

Second Example, results

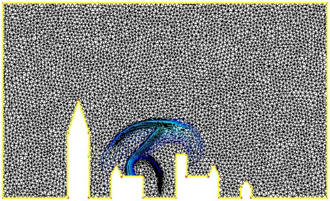

Second Example, results

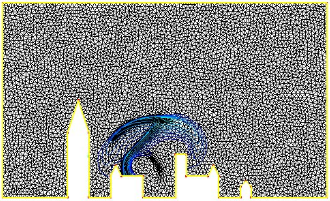

Second Example, results

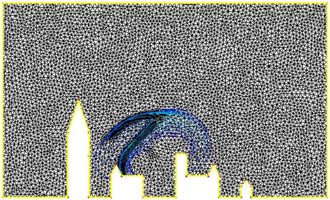

Second Example, results

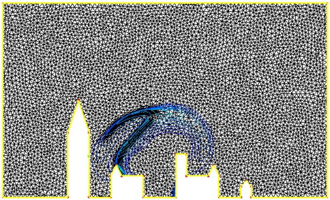

Second Example, results

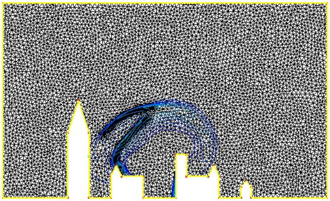

Second Example, results

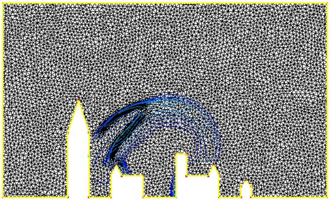

Second Example, results

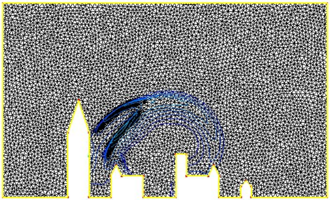

Second Example, results

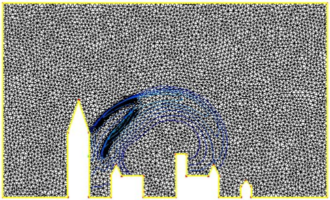

Second Example, results

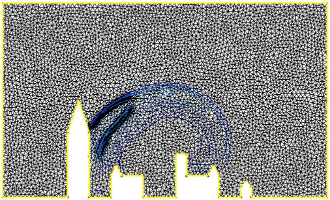

Second Example, results

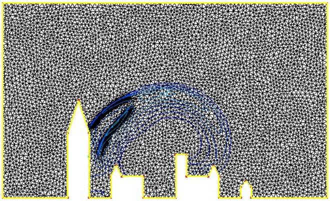

- For acoustic analysis, the use of anisotropic meshes seems less mandatory.
- Uniform meshes allow a higher accuracy with lower cost per node, but need good absorbing boundaries.
- For a particular family of problems, noise emission and noise observation ("micro") are locallised in a small portion of the domain and much resolution can be useless.
- In that case, the goal-oriented formulation helps focalising the mesh effort on the propagation from source to micro.

Comparison between Goal-Oriented approach and multiscale L^p:

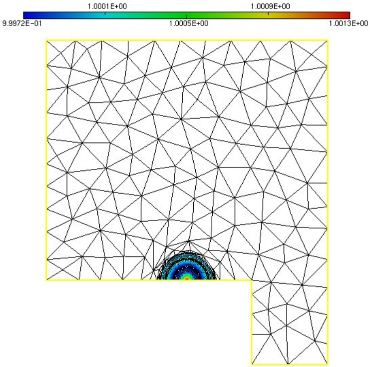

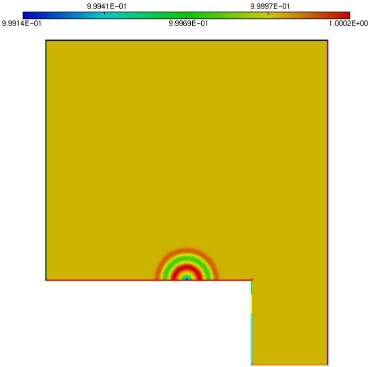

Comparison between Goal-Oriented approach and multiscale L^p:

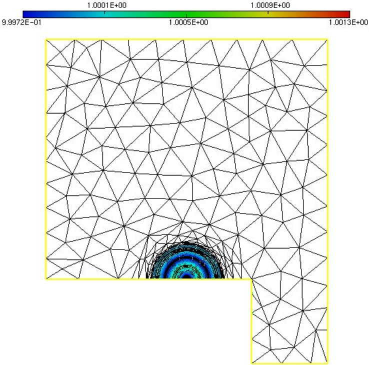

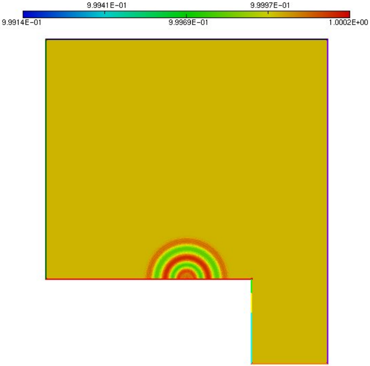

Comparison between Goal-Oriented approach and multiscale L^p:

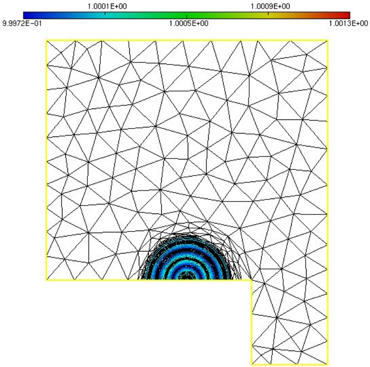

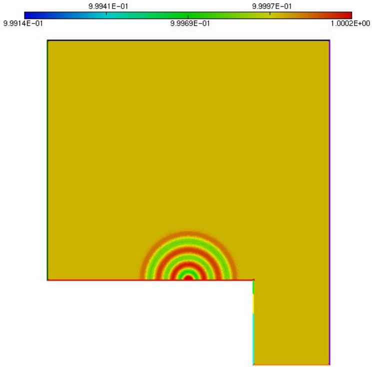

Application to acoustics

Comparison between Goal-Oriented approach and multiscale L^p:

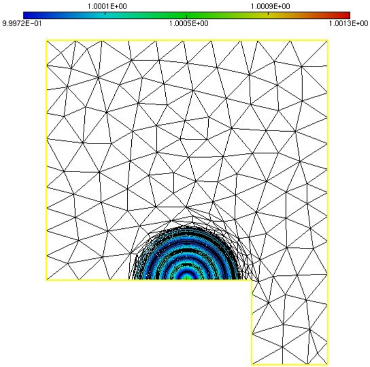

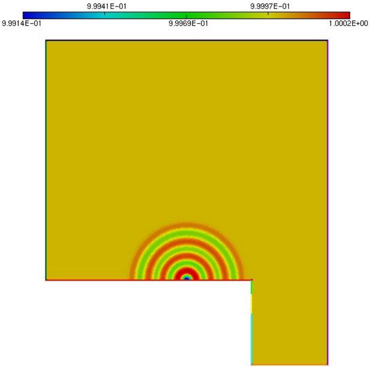

Comparison between Goal-Oriented approach and multiscale L^p:

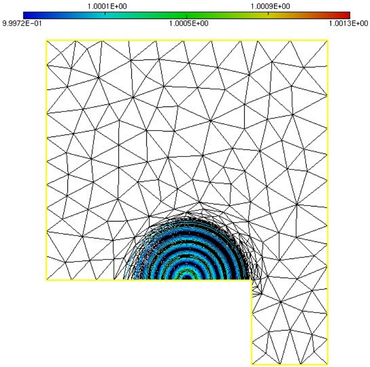

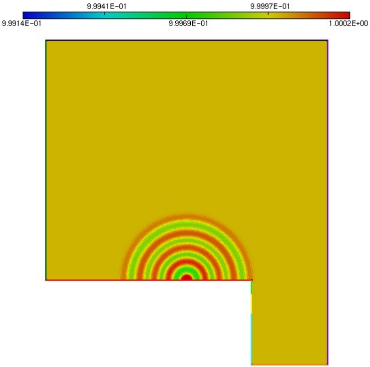

Comparison between Goal-Oriented approach and multiscale L^p:

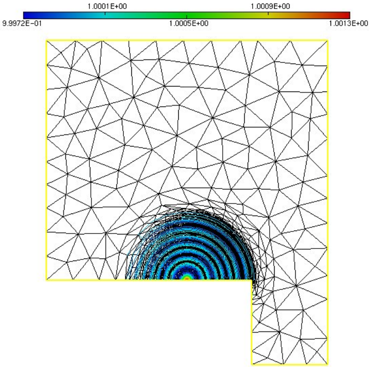

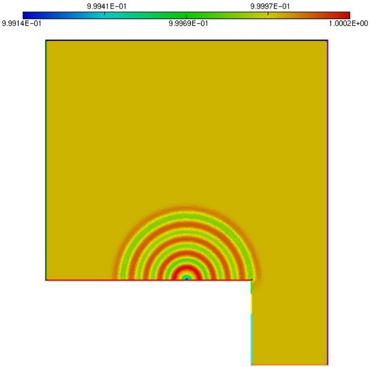

Comparison between Goal-Oriented approach and multiscale L^p:

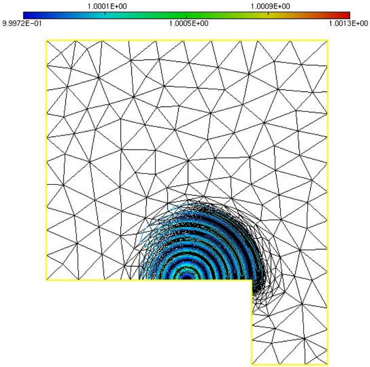

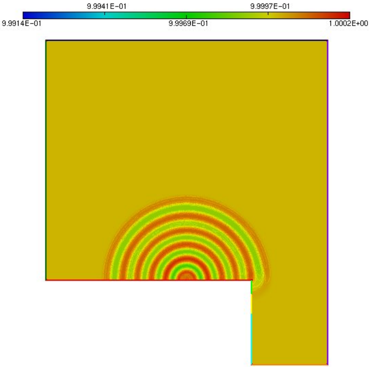

Application to acoustics

Comparison between Goal-Oriented approach and multiscale L^p:

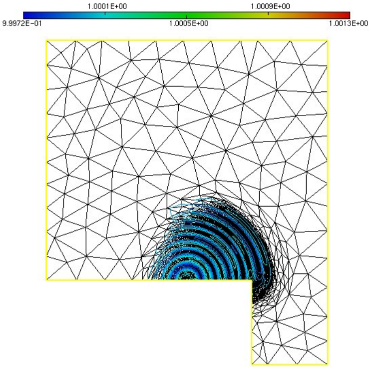

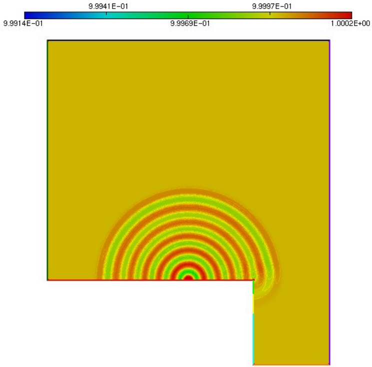

Comparison between Goal-Oriented approach and multiscale L^p:

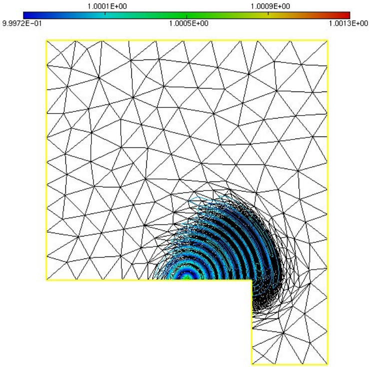

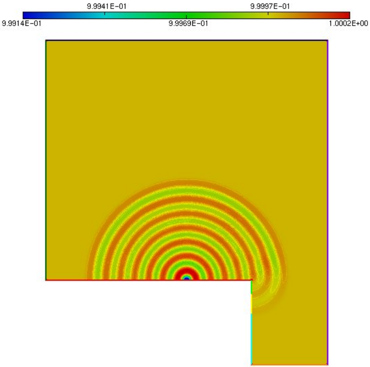

Comparison between Goal-Oriented approach and multiscale L^p:

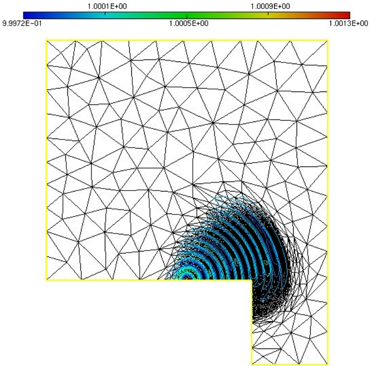

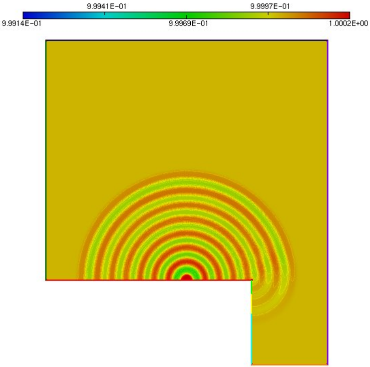

Comparison between Goal-Oriented approach and multiscale L^p:

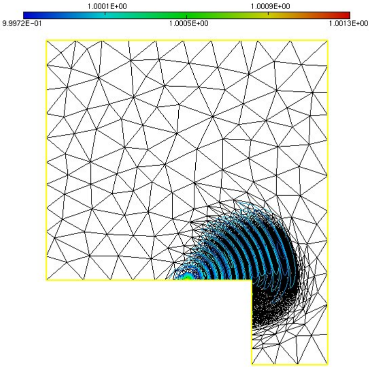

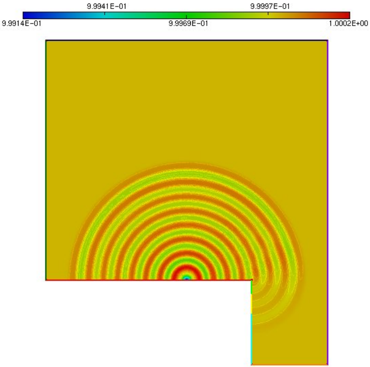

Comparison between Goal-Oriented approach and multiscale L^p:

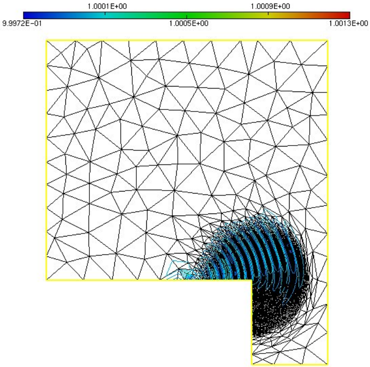

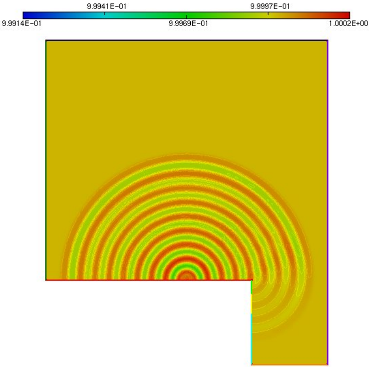

Comparison between Goal-Oriented approach and multiscale L^p:

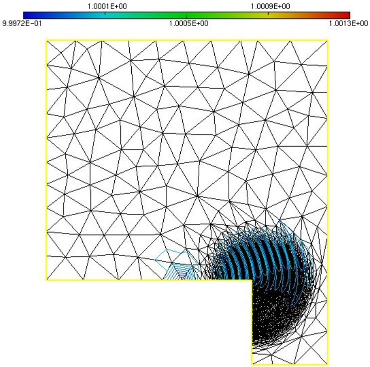

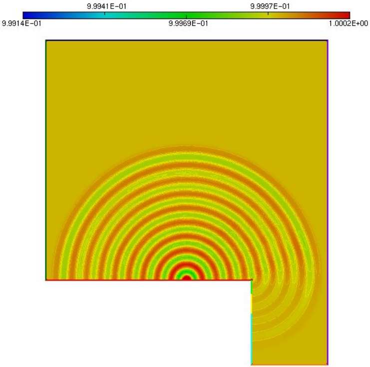

Comparison between Goal-Oriented approach and multiscale L^p:

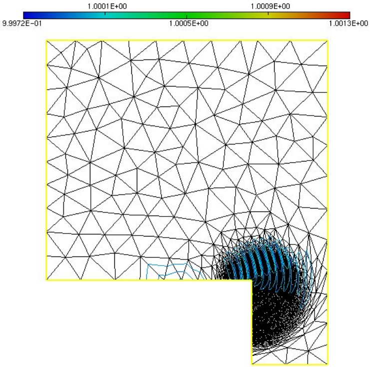

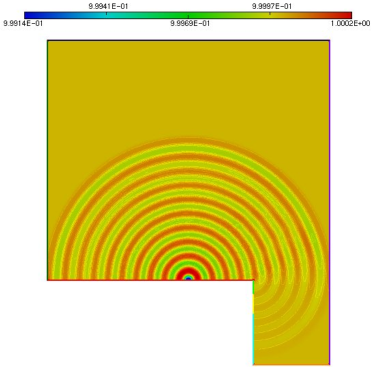

Application to acoustics

Comparison between Goal-Oriented approach and multiscale L^p:

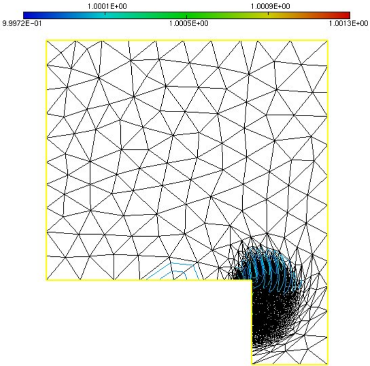

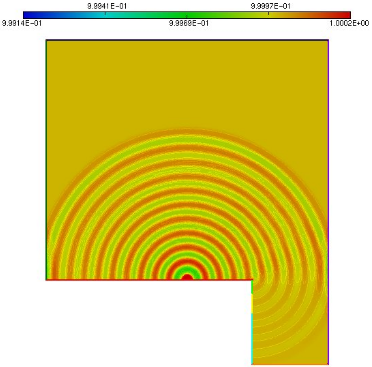

Application to acoustics

Comparison between Goal-Oriented approach and multiscale L^p:

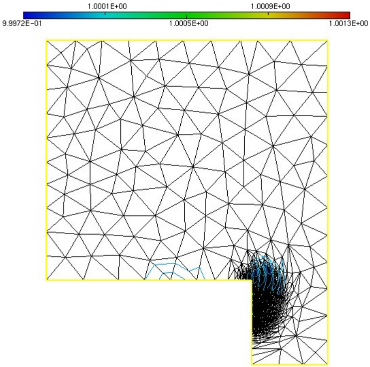

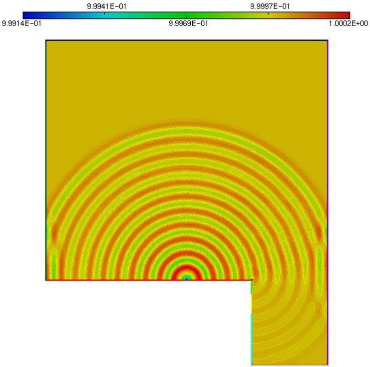

Comparison between Goal-Oriented approach and multiscale L^p:

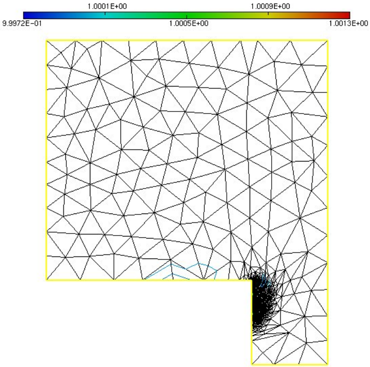

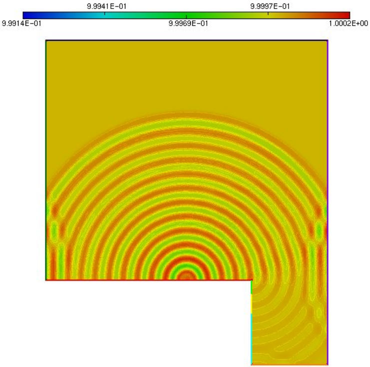

Comparison between Goal-Oriented approach and multiscale L^p:

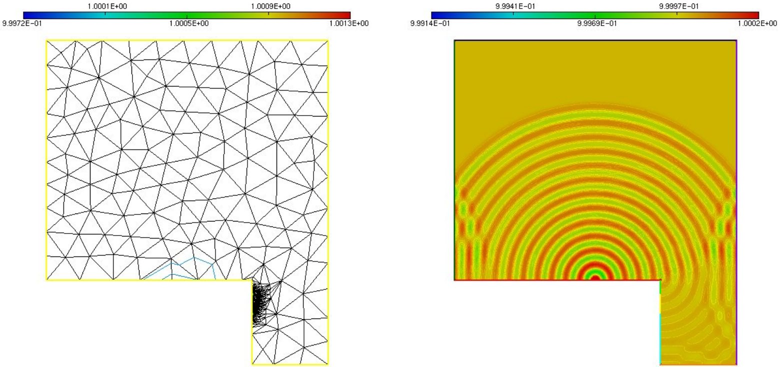

Application to acoustics

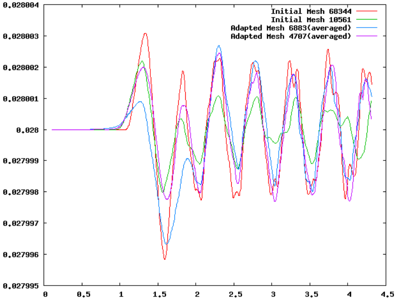

Application to 2D acoustics(2)

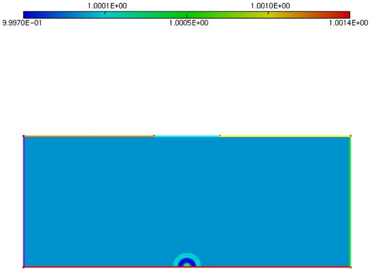

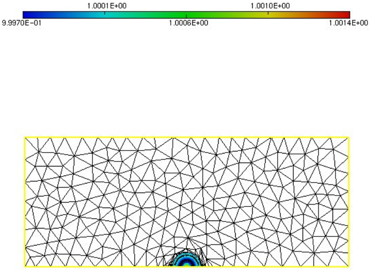

Application to 2D acoustics(2)

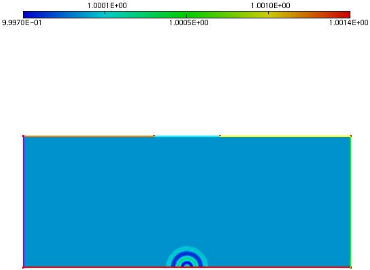

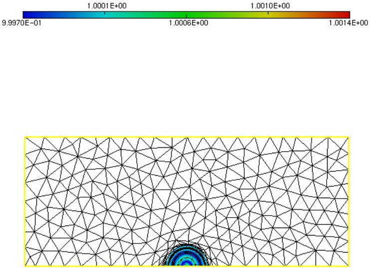

Application to 2D acoustics(2)

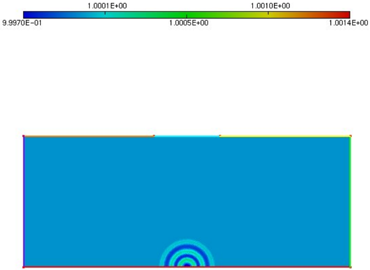

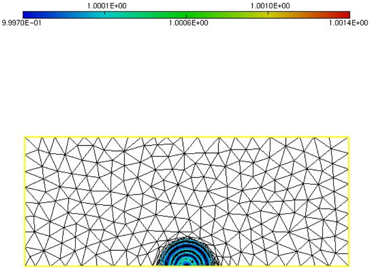

Application to 2D acoustics(2)

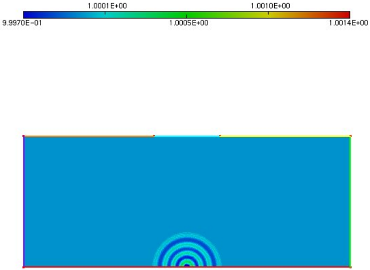

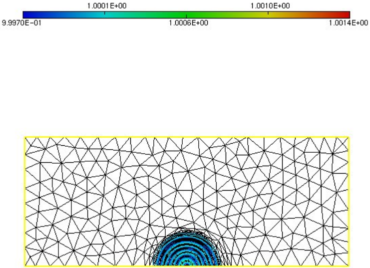

Application to 2D acoustics(2)

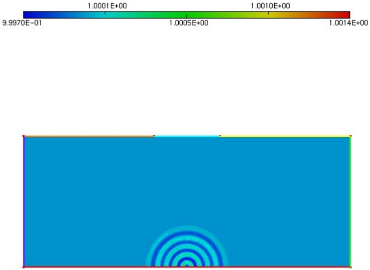

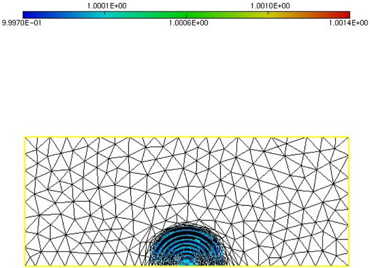

Application to 2D acoustics(2)

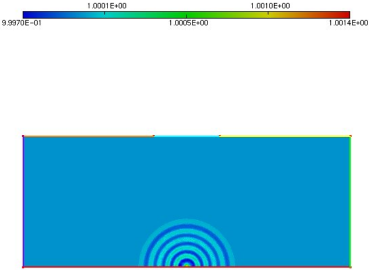

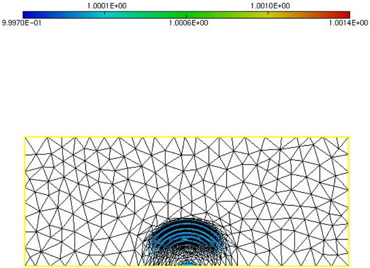

Application to 2D acoustics(2)

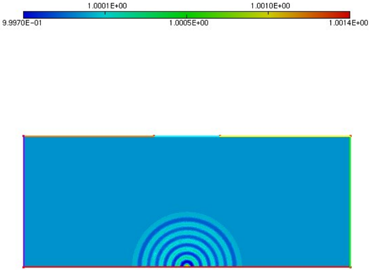

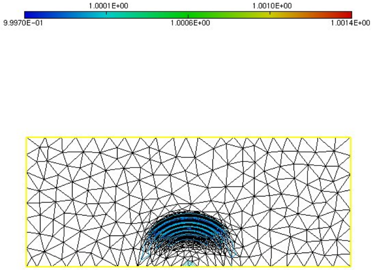

Application to 2D acoustics(2)

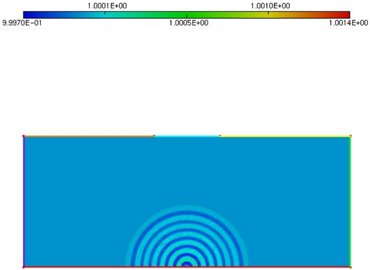

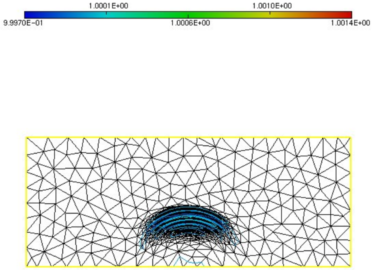

Application to 2D acoustics(2)

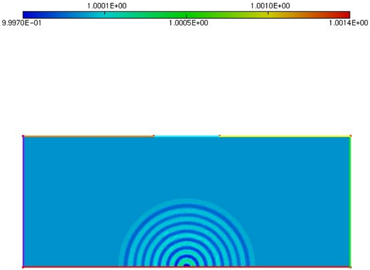

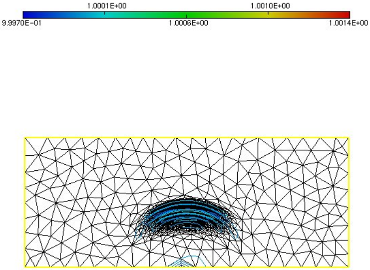

Application to 2D acoustics(2)

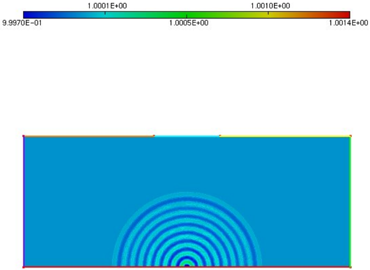

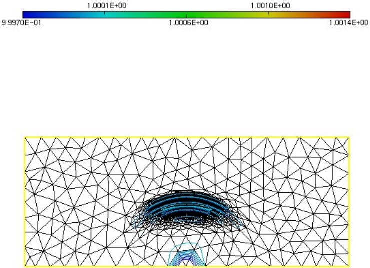

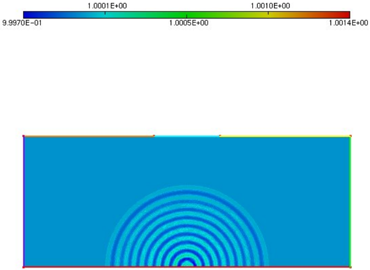
1.0001E+00
1.0010E+00
9.9970E-01
1.0005E+00
1.0014E+00

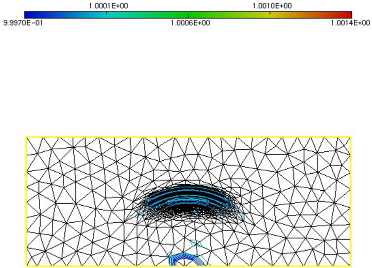
1.0001E+00
1.0010E+00
9.9970E-01
1.0006E+00
1.0014E+00

Application to 2D acoustics(2)

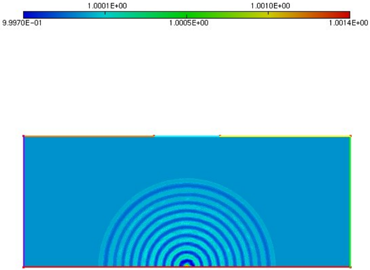

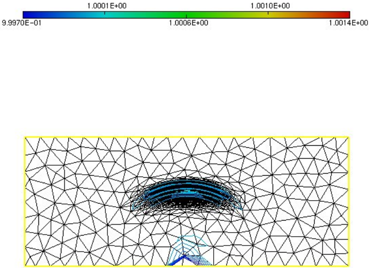

Application to 2D acoustics(2)

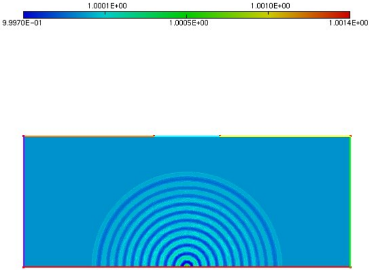

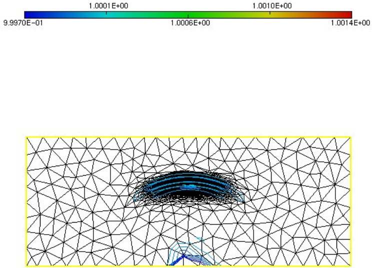

Application to 2D acoustics(2)

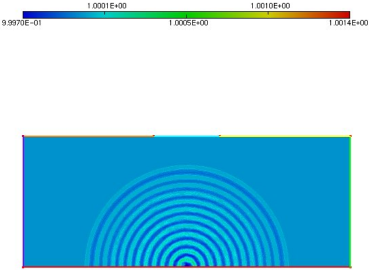

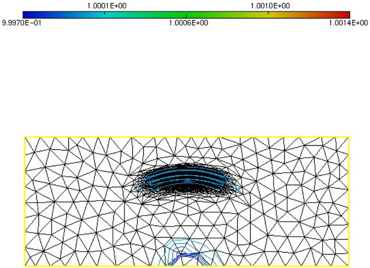

Application to 2D acoustics(2)

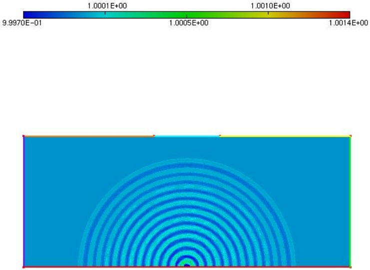

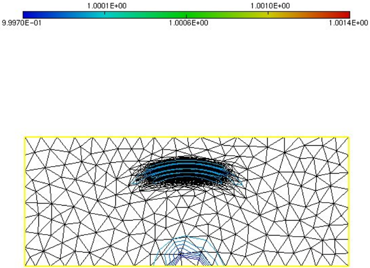

Application to 2D acoustics(2)

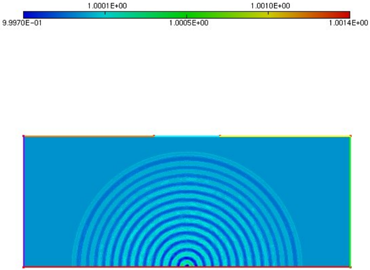

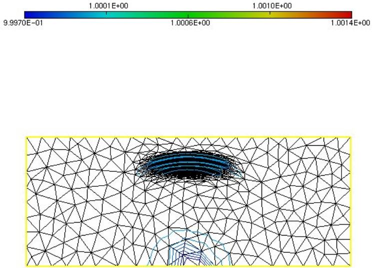

Application to 2D acoustics(2)

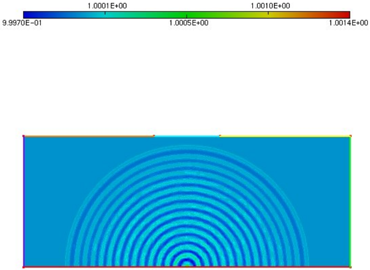

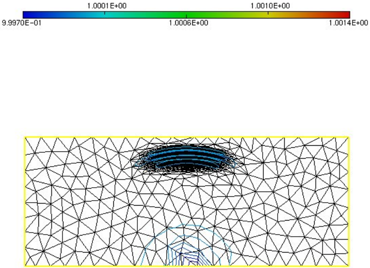

Application to 2D acoustics(2)

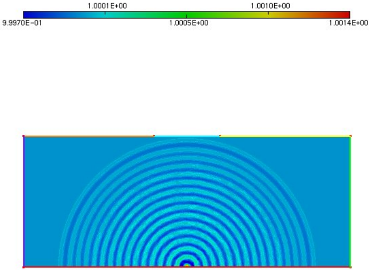

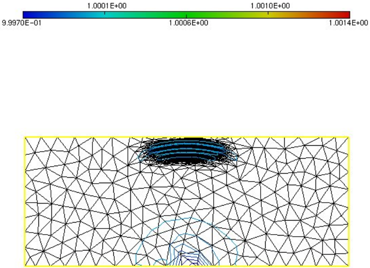

Application to 2D acoustics(2)

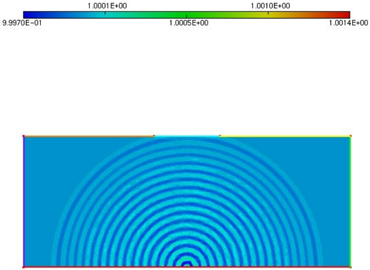

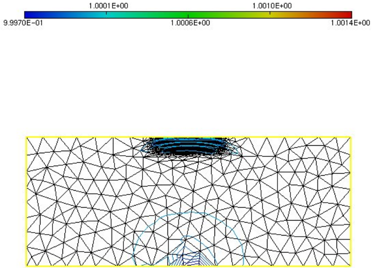

Application to 2D acoustics(2)

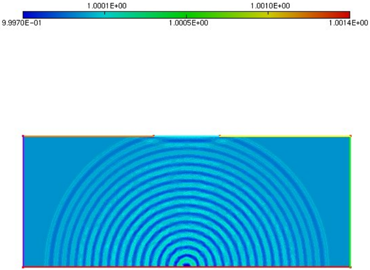

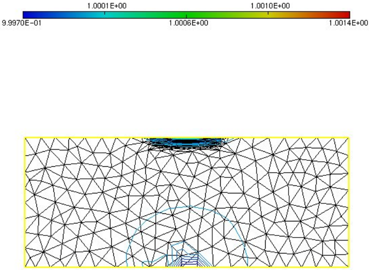

Application to 2D acoustics(2)

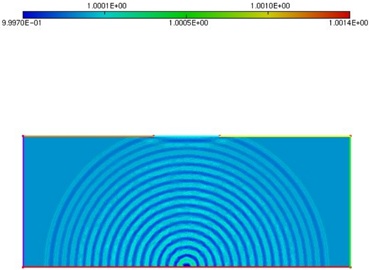

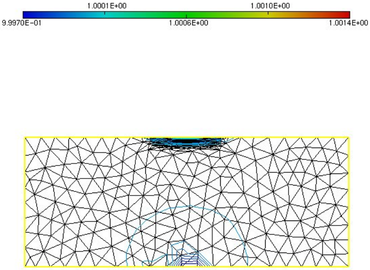

Conclusion:

- New mesh adaptation algorithm which prescribes the spatial mesh of an unsteady simulation as the optimum of a goal-oriented error analysis;
- Extension to unsteadiness is applied in an implicit mesh-solution coupling which needs a non-linear iteration, the fixed point;
- The new algorithm is applied to a blast wave test case and a noise propagation test case and shows on these calculations the favourable behavior expected from an adjoint-based method (automatic selection of the mesh necessary for the target output)

Perpectives:

- Accurate integration of time errors in the mesh adaptation process with a more general formulation of the mesh optimisation problem (work in progress)
- Higher order adjoint schemes and 3D unsteady test-cases (work in progress)
- Application to turbulent aeroacoustics (3D Navier-Stokes equations)